

One-step implementation of the genuine Fredkin gate in high- Q coupled three-cavity arrays

Xiao-Qiang Shao^{*,1,2} Tai-Yu Zheng,¹ Xun-Li Feng,² C. H. Oh,² and Shou Zhang³

¹*School of Physics, Northeast Normal University Changchun 130024, People's Republic of China*

²*Centre for Quantum Technologies, National University of Singapore, 3 Science Drive 2, Singapore 117543*

³*Department of Physics, College of Science, Yanbian University, Yanji, Jilin 133002, People's Republic of China*

We present two efficient methods for implementing the Fredkin gate with atoms separately trapped in an array of three high- Q coupled cavities. The first proposal is based on the resonant dynamics, which leads to a fast resonant interaction in a certain subspace while leaving others unchanged, and the second one utilizes a dispersive interaction such that the effective long-distance dipole-dipole interaction between two distributed target qubits is achieved by virtually excited process. Both schemes can achieve the standard form of the Fredkin gate in a single step without any subsequent single-qubit operation. The effects of decoherence on the performance of the gate are also analyzed in virtue of master equation, and the strictly numerical simulation reveals that the average fidelity of the quantum gate is high.

PACS numbers: 03.67.-a, 03.67.Lx, 42.50.Pq

I. INTRODUCTION

The quantum mechanics based computers can outperform traditional computers by a far greater order of magnitude in computing power, because they permit parallel computation due to the principle of superposition and entanglement [1–3]. In a quantum computer, the quantum logic gates constitute the basic building blocks of quantum circuit which are reversible transformations on an n -qubit register. According to the principle of universal quantum computation, any unitary operation can be decomposed into a series of single qubit operations along with two-qubit gates [4], e.g. achievement of a generic two-qubit gate may require a sequence of up to three CNOT gates combined with single-qubit rotations. Nevertheless, this kind of decomposition becomes inefficient as applied to a multi-qubit (three or more) gate, for the procedure will become more complicated and makes the quantum system further susceptible to the environment. Therefore, much attention has been paid on the direct implementation of multi-qubit gates both in theory and experiment [5–16].

$$U_{\text{FRED}} = \begin{bmatrix} 1 & 0 & 0 & 0 & 0 & 0 & 0 & 0 \\ 0 & 1 & 0 & 0 & 0 & 0 & 0 & 0 \\ 0 & 0 & 1 & 0 & 0 & 0 & 0 & 0 \\ 0 & 0 & 0 & 1 & 0 & 0 & 0 & 0 \\ 0 & 0 & 0 & 0 & 1 & 0 & 0 & 0 \\ 0 & 0 & 0 & 0 & 0 & 1 & 0 & 0 \\ 0 & 0 & 0 & 0 & 0 & 0 & 1 & 0 \\ 0 & 0 & 0 & 0 & 0 & 0 & 0 & 1 \end{bmatrix}. \quad (1)$$

The Fredkin gate [17], together with Toffoli gate becomes the important logic gate in the domain of three-qubit gates. Its matrix form expanded in subspace

$\{|0_2\rangle, |1_2\rangle, |0_1\rangle, |1_1\rangle, |0_3\rangle, |1_3\rangle\}$ is shown in Eq. (1), from which we see two target qubits swap their information $|01\rangle_{1,3} \Leftrightarrow |10\rangle_{1,3}$ if and only if the control qubit is in $|1_2\rangle$. This gate not only has been useful in designing a circuit for error correcting quantum computations [18], but also has given a simple implementation of the quantum computer to solve Deutsch's problem [19]. Since the first quantum optical Fredkin gate was proposed in theory by Milburn [20], the physical realization of Fredkin gate has flourished in the field of linear optics in recent years. Fiurášek suggested a heralded Fredkin gate that used ancilla photons, interference, and single-photon detection to emulate the cross-Kerr nonlinearity [21], then the author put forward an alternative scheme for linear optical quantum Fredkin gate based on the combination of recently experimentally demonstrated linear optical partial-SWAP gate and controlled-Z gates [22]. Gong *et al.* presented two methods for a linear optical quantum Fredkin gate with only linear optics and single photons [23]. Lin *et al.* realized the Fredkin gate with weak cross-Kerr nonlinearity based on the controlled-path gate [24]. The prominent merit of linear-optical technique is that photons is best for the quantum information process due to its weak interaction with the environment, but the low success probability may restraint the development of large-scale quantum computation. It is worth noting that Ref. [25] presented a simple architecture for deterministic quantum circuits operating on single photon qubits. The research about the deterministic Fredkin gate initiated in several hybrid quantum systems, e.g. ion-phonon in a two-dimensional ion trap [26] and atom-photon via the cavity input-output process [27, 28]. However, the different representations of qubits do not agree with the requirement for quantum computing as a typical quantum algorithm may require each qubit to be treated equally. Although there are certain schemes that simulate Fredkin gate operation in cavity QED system [29] and superconduction system [30], either extra ancillary levels need to

*E-mail: xqshao@yahoo.com

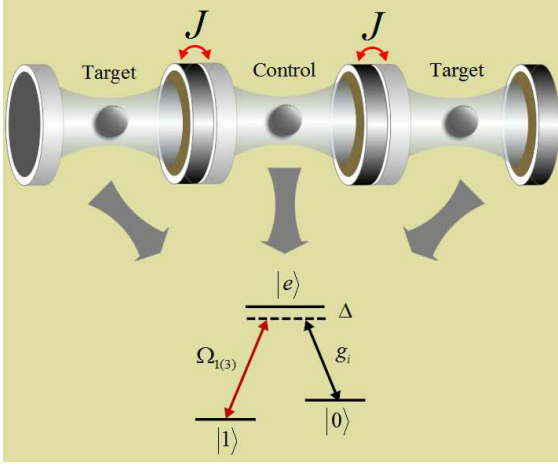


FIG. 1: (Color online) Schematic of three atoms trapped in three coupled cavities. Each qubit is encoded into two lower-energy levels labeled as $|0\rangle$ and $|1\rangle$. The transitions between the levels $|e_i\rangle \leftrightarrow |0_i\rangle$ is coupled to the cavity mode with the coupling constants g_i , and the transitions $|e_{1(3)}\rangle \leftrightarrow |1_{1(3)}\rangle$ is driven by a classical pulse with the Rabi frequencies $\Omega_{1(3)}$. Δ represents the corresponding one-photon detuning parameter and the photon can hop between two cavities with coupling strength J . The atom in the middle cavity serves as the control qubit while the atoms in bilateral cavities play the role of the target qubits, and we label the atoms as 1, 2, 3 from left to right for convenience, and the state $|\alpha_1, \beta_2, \gamma_3\rangle_a$ is abbreviated to $|\alpha, \beta, \gamma\rangle_a$ in the text.

be introduced or local operations should be applied.

Coupled-cavity models describe a series of optical cavities, each containing one or more atoms with photons permitted to hop between neighboring cavities. The original purpose for introducing coupled-cavity models is to overcome the problem of individual addressability. Along with theoretically intensive study on this model, many interesting phenomena are observed such as photon blockade induced Mott transitions [31], polaritonic characteristics of insulator and superfluid states [32], fractional quantum Hall state [33], multimode entanglement [34], and other quantum many-body phenomena [35]. Recently, the coupled-cavity systems are also applied in distributed controlled-phase gate [36–39]. In this paper, we explore the particular feature in coupled three-cavity array system and propose two efficient schemes for implementing the genuine Fredkin gate in a coupled-cavity array. Compared with previous proposals, the advantages of ours are threefold: (i) the quantum information is encoded into three identical atoms without introducing any ancillary level, which satisfies the requirement for quantum computation; (ii) the qubits are trapped separately in three cavities, and this arrangement will make it convenient to control and measure qubit individually; (iii) the Fredkin gate is fast achieved for it only needs one-step operation dispense with any single qubit gate. In particular, the present scheme provide two options for achieving high-fidelity quantum gate without resorting to

non-identical coupling adopted in Ref [30].

The structure of the paper is as follows. In Sec. 2, we derive the effective Hamiltonians that govern the evolution of quantum states for the resonant- and dispersive interaction between atom and coupled cavity, respectively. In Sec. 3, we discuss the performance of the scheme via the definition of average fidelity for quantum logic gate and consider the effect of typical decoherence in virtue of master equation. Then a summary appears in Sec. 4.

II. EFFECTIVE HAMILTONIAN IN COUPLED-CAVITY ARRAY SYSTEM

The considered physical system consists of three atoms with Λ -type configuration trapped in a coupled-cavity array, as shown in Fig. 1. Each atom interacts with cavity mode via the Jaynes-Cummings (JC) model, where the transitions between the levels $|e_i\rangle \leftrightarrow |0_i\rangle$ are coupled to the cavity mode with the coupling constants g_i . In addition, we apply two classical fields to drive the atomic transitions $|e_1\rangle \leftrightarrow |1_1\rangle$ and $|e_3\rangle \leftrightarrow |1_3\rangle$, respectively. The corresponding one-photon detuning parameter is Δ and the photon can hop between two neighbor cavities with coupling strength J . The Hamiltonian of the system in the Schrödinger picture reads ($\hbar = 1$)

$$\begin{aligned}
 H_S = & \sum_{j=1,3} \Omega_j (|e_j\rangle\langle 1_j| e^{-i\omega_j^j t} + |1_j\rangle\langle e_j| e^{i\omega_j^j t}) \\
 & + \sum_{k=1}^2 J (a_k^\dagger a_{k+1} + a_k a_{k+1}^\dagger) \\
 & + \sum_{i=1}^3 g_i (a_i |e_i\rangle\langle 0_i| + |0_i\rangle\langle e_i| a_i^\dagger) + \sum_{k=1}^3 \omega_c a_k^\dagger a_k \\
 & + \sum_{i=1}^3 \omega_e |e_i\rangle\langle e_i| + \omega_0 |0_i\rangle\langle 0_i| + \omega_1 |1_i\rangle\langle 1_i|, \quad (2)
 \end{aligned}$$

where ω_j^j is the frequency of j th classical field, ω_c denotes the cavity frequency and $\omega_{e(0,1)}$ represents the energy of atomic level $|e\rangle(|0\rangle, |1\rangle)$. In the interaction picture, after performing a rotating with respect to $U = \exp(i\Delta t \sum_{i=1}^3 |e_i\rangle\langle e_i|)$, the Hamiltonian can be written as

$$\begin{aligned}
 H_I = & \sum_{j=1,3} \Omega_j (|e_j\rangle\langle 1_j| + |1_j\rangle\langle e_j|) + \sum_{k=1}^2 J (a_k^\dagger a_{k+1} \\
 & + a_k a_{k+1}^\dagger) + \sum_{i=1}^3 g_i (a_i |e_i\rangle\langle 0_i| + |0_i\rangle\langle e_i| a_i^\dagger) \\
 & + \Delta |e_i\rangle\langle e_i|. \quad (3)
 \end{aligned}$$

The last term in Eq. (3) plays an important role in our scheme because the presence of Δ or not determines the dynamics to be resonant or dispersive. In what follows, we will discuss the possibility for one-step achieving the genuine Fredkin with the mentioned dynamics in detail.

A. Resonant interaction between cavity and doped atom

In this section, we focus on synthesizing the Fredkin gate with the resonant interaction. The system we consider is a simplification of Fig. 1 ($\Delta = 0$), i.e. the atom in each cavity is resonantly coupled to the cavity field and the classical field. Before preceding, we first divide the Hamiltonian of Eq. (3) into two parts as analogous to quantum Zeno dynamics [40]:

$$\begin{aligned} H_I &= H_1 + H_2, \\ H_1 &= \sum_{j=1,3} \Omega_j (|e_j\rangle\langle 1_j| + |1_j\rangle\langle e_j|), \\ H_2 &= \sum_{k=1}^2 J(a_k^\dagger a_{k+1} + a_k a_{k+1}^\dagger) + \sum_{i=1}^3 g_i (a_i |e_i\rangle\langle 0_i| \\ &\quad + |0_i\rangle\langle e_i| a_i^\dagger), \end{aligned} \quad (4)$$

where H_1 is the Hamiltonian of the system to be investigated and H_2 can be considered as an additional interaction Hamiltonian performing the “measurement”. For a large ratio $g/\Omega_{1(3)}(J/\Omega_{1(3)})$, the system investigated can be viewed as dominated by the evolution operator $\mathcal{U}(t) = \exp(iH_2 t)U_I^e(t)$, which can be shown to have the form $\mathcal{U}(t) = \exp(-iH_Z t)$, where $H_Z = \sum_n P_n H_1 P_n$, is called Zeno Hamiltonian, P_n being the eigenprojection of H_2 belonging to the eigenvalue η_n , and $H_2 = \sum_n \eta_n P_n$, thus the total Hamiltonian reads

$$H_{eff}^e = \sum_n \eta_n P_n + P_n H_1 P_n. \quad (5)$$

If the interested quantum system is freezed to the dark subspace ($n = 0$) of H_2 , the whole system are governed by the effective Hamiltonian

$$H_{eff}^e = P_0 H_1 P_0. \quad (6)$$

For three-qubit logic gate, there are eight input states needed to be computed in subspace $\{|0_1\rangle, |1_1\rangle, |0_2\rangle, |1_2\rangle, |0_3\rangle, |1_3\rangle\}$. Since the JC model Hamiltonian of atom and coupled cavity conserves the excitation number $\mathcal{N}_k = a_k^\dagger a_k + |e_k\rangle\langle e_k|$, it is convenient to reclassify the above bases in different excitation subspaces, i.e. $\{|000\rangle_a|000\rangle_c, |010\rangle_a|000\rangle_c\}$ belong to the “zero excitation” subspace, $\{|001\rangle_a|000\rangle_c, |100\rangle_a|000\rangle_c\}$ and $\{|011\rangle_a|000\rangle_c, |110\rangle_a|000\rangle_c\}$ correspond to two independent “single excitation” subspaces, and $\{|101\rangle_a|000\rangle_c\}$ and $\{|111\rangle_a|000\rangle_c\}$ are included in two different “two excitation” subspaces. The primary function of a Fredkin gate is to perform the controlled swap operation $|1\rangle_C|0\rangle_T \Leftrightarrow |1\rangle_C|10\rangle_T$, thereby the dynamical evolutions of $\{|011\rangle_a|000\rangle_c, |110\rangle_a|000\rangle_c\}$ are investigated first.

In the closed subspace $\{|011\rangle_a|000\rangle_c, |01e\rangle_a|000\rangle_c, |010\rangle_a|001\rangle_c, |010\rangle_a|010\rangle_c, |010\rangle_a|100\rangle_c, |e10\rangle_a|000\rangle_c,$

$|110\rangle_a|000\rangle_c\}$, we can expand Hamiltonian of Eq. (3) as

$$M^{re} = \begin{bmatrix} 0 & \Omega_3 & 0 & 0 & 0 & 0 & 0 \\ \Omega_3 & 0 & g & 0 & 0 & 0 & 0 \\ 0 & g & 0 & J & 0 & 0 & 0 \\ 0 & 0 & J & 0 & J & 0 & 0 \\ 0 & 0 & 0 & J & 0 & g & 0 \\ 0 & 0 & 0 & 0 & g & 0 & \Omega_1 \\ 0 & 0 & 0 & 0 & 0 & \Omega_1 & 0 \end{bmatrix}. \quad (7)$$

The eigenprojection operator P_n of atom-cavity interaction can be constructed from $|E_1\rangle = \frac{1}{\sqrt{3}}(|e10\rangle_a|000\rangle_c + |01e\rangle_a|000\rangle_c - |010\rangle_a|010\rangle_c)$, $|E_2\rangle = \frac{1}{2}[(|e10\rangle_a - |01e\rangle_a)|000\rangle_c - |010\rangle_a(|100\rangle_c - |001\rangle_c)]$, $|E_3\rangle = \frac{1}{2}[(|e10\rangle_a - |01e\rangle_a)|000\rangle_c + |010\rangle_a(|100\rangle_c - |001\rangle_c)]$, $|E_4\rangle = -\frac{1}{\sqrt{12}}(|e10\rangle_a + |01e\rangle_a)|000\rangle_c + \frac{1}{2\sqrt{3}}|010\rangle_a(\sqrt{3}|100\rangle_c + \sqrt{3}|001\rangle_c - 2|010\rangle_c)$, and $|E_5\rangle = \frac{1}{\sqrt{12}}(|e10\rangle_a + |01e\rangle_a)|000\rangle_c + \frac{1}{2\sqrt{3}}|010\rangle_a(\sqrt{3}|100\rangle_c + \sqrt{3}|001\rangle_c + 2|010\rangle_c)$ corresponding to the eigenvalues $E_1 = 0$, $E_2 = -g$, $E_3 = g$, $E_4 = -\sqrt{3}g$, and $E_5 = \sqrt{3}g$, where we have assumed $J = g$ for simplicity. Thus the Eq. (7) can be rewritten as

$$\begin{aligned} H_{re} &= \Omega_1 |110\rangle_a|000\rangle_c \left[\frac{1}{\sqrt{3}}\langle E_1| + \frac{1}{2}(\langle E_2| + \langle E_3|) \right. \\ &\quad \left. - \frac{1}{\sqrt{12}}(\langle E_4| - \langle E_5|) \right] + \Omega_3 |011\rangle_a|000\rangle_c \left[\frac{1}{\sqrt{3}}\langle E_1| \right. \\ &\quad \left. - \frac{1}{2}(\langle E_2| + \langle E_3|) - \frac{1}{\sqrt{12}}(\langle E_4| - \langle E_5|) \right] \\ &\quad + \text{H.c.} + \sum_{i=1}^5 E_i |E_i\rangle\langle E_i|. \end{aligned} \quad (8)$$

Eq. (8) describes that $|110\rangle_a|000\rangle_c$ and $|011\rangle_a|000\rangle_c$ couple to excitation state $|E_i\rangle$ with detuning E_i , respectively. Thus under a strong continuous coupling $g \gg |\Omega_{1(3)}|$, we may neglect the large detuned terms and the dominant part that governs the evolution of quantum states in this subspace reduces to the resonant coupling with detuning $E_1 = 0$, i.e.

$$H_{eff}^e = \frac{1}{\sqrt{3}}(\Omega_1 |110\rangle_a + \Omega_3 |011\rangle_a) |000\rangle_c |D\rangle + \text{H.c.}, \quad (9)$$

where we have relabeled $|E_1\rangle$ as $|D\rangle$ for it is immune to the interaction between atoms and coupled-cavity array.

According to Eq. (6), we find other input states do not participate in the dynamical evolution at the requirement of Zeno condition $|\Omega_{1(3)}| \ll g$. Therefore a genuine Fredkin gate can be carried out in one step as

$$\int_0^T \frac{1}{\sqrt{3}} \Omega dt = \frac{\pi}{\sqrt{2}}, \quad (\Omega_1 = -\Omega_3 = \Omega). \quad (10)$$

We may control two Rabi frequencies of classical fields adiabatically as [41]

$$\Omega(t) = 2\Omega_{max} \sin^2 \left[\sqrt{\frac{2}{3}} \Omega_{max} t \right], \quad (11)$$

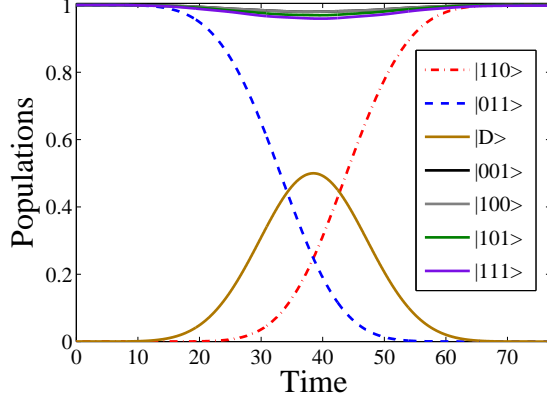


FIG. 2: (Color online) Evolutions for the populations of interested states. The qubit states $|011\rangle_a|000\rangle_c$ and $|110\rangle_a|000\rangle_c$ coherently transform into each other via the media state $|D\rangle$, while other qubit states are frozen to their original status due to the large detuned interaction. The corresponding parameters are $J = g$ and $\Omega_{max} = 0.05g$.

and this choice corresponds to the interaction time $T = \sqrt{3}\pi/(\sqrt{2}\Omega_{max})$. In Fig. 2, we depict the time evolution of each input state during the gate operation process with the full Hamiltonian of Eq. (3). We find the Zeno condition $|\Omega_{1(3)}| \ll g$ guarantees the effectiveness of Eq. (9) well and an adiabatic evolution of quantum gate makes the scheme more stable, because the populations of states $|011\rangle_a|000\rangle_c$ and $|110\rangle_a|000\rangle_c$ keep maximal in a period of time instead of one spot. The prominent advantage of the present scheme is that the Fredkin gate is achieved in a short time due to the resonant interaction between coupled-cavity array and doped atom, but the dark state $|D\rangle$ still incorporates the excited state of atoms and the middle cavity, which may cause the quantum gate to be sensitive to the decoherence. In next section, we will modify the above scheme and resort to another method for implementing the Fredkin gate in a dispersive way.

B. Dispersive interaction between cavity and doped atom

In this section, we discuss the possibility of achieving the Fredkin gate via dispersive interaction between atom and coupled cavity. The analysis still relies on the idea of quantum Zeno dynamics, nevertheless, more input states should be considered since the complicated dynamics induced by Δ . For the subspace $\{|100\rangle_a|000\rangle_c, |001\rangle_a|000\rangle_c, |000\rangle_a|100\rangle_c, |000\rangle_a|010\rangle_c, |000\rangle_a|001\rangle_c, |e00\rangle_a|000\rangle_c, |0e0\rangle_a|000\rangle_c, |00e\rangle_a|000\rangle_c\}$, we need to introduce the following collective cavity states $|\varphi_a\rangle = \frac{1}{2}|000\rangle_a(|100\rangle - \sqrt{2}|010\rangle + |001\rangle)_c$, $|\varphi_b\rangle = \frac{1}{2}|000\rangle_a(|100\rangle + \sqrt{2}|010\rangle + |001\rangle)_c$, $|\varphi_c\rangle = \frac{1}{\sqrt{2}}|000\rangle_a(|100\rangle - |001\rangle)_c$, and collective atomic states $|\varphi_1\rangle = \frac{1}{2}(|e00\rangle - \sqrt{2}|0e0\rangle + |00e\rangle)_a|000\rangle_c$, $|\varphi_2\rangle = \frac{1}{2}(|e00\rangle +$

$\sqrt{2}|0e0\rangle + |00e\rangle)_a|000\rangle_c$, $|\varphi_3\rangle = \frac{1}{\sqrt{2}}(|e00\rangle - |00e\rangle)_a|000\rangle_c$. In the new basis $\{|\varphi_1\rangle, |\varphi_a\rangle, |\varphi_2\rangle, |\varphi_b\rangle, |\varphi_3\rangle, |\varphi_c\rangle\}$, the Hamiltonian of atom-cavity interaction is simplified to the form of three 2×2 block matrices:

$$M^{de} = \begin{bmatrix} \Delta & g & 0 & 0 & 0 & 0 \\ g & -\sqrt{2}J & 0 & 0 & 0 & 0 \\ 0 & 0 & \Delta & g & 0 & 0 \\ 0 & 0 & g & \sqrt{2}J & 0 & 0 \\ 0 & 0 & 0 & 0 & \Delta & g \\ 0 & 0 & 0 & 0 & g & 0 \end{bmatrix}, \quad (12)$$

and this matrix can be solved easily of which the eigenvalues are

$$\begin{aligned} E_1 &= \frac{1}{2} \left(\Delta - \sqrt{2}J - \sqrt{4g^2 + \Delta^2 + 2\sqrt{2}\Delta J + 2J^2} \right), \\ E_2 &= \frac{1}{2} \left(\Delta - \sqrt{2}J + \sqrt{4g^2 + \Delta^2 + 2\sqrt{2}\Delta J + 2J^2} \right), \\ E_3 &= \frac{1}{2} \left(\Delta + \sqrt{2}J - \sqrt{4g^2 + \Delta^2 - 2\sqrt{2}\Delta J + 2J^2} \right), \\ E_4 &= \frac{1}{2} \left(\Delta + \sqrt{2}J + \sqrt{4g^2 + \Delta^2 - 2\sqrt{2}\Delta J + 2J^2} \right), \\ E_5 &= \frac{1}{2} \left(\Delta - \sqrt{4g^2 + \Delta^2} \right), \\ E_6 &= \frac{1}{2} \left(\Delta + \sqrt{4g^2 + \Delta^2} \right), \end{aligned} \quad (13)$$

corresponding to the eigenstates

$$\begin{aligned} |E_1\rangle &= \frac{\alpha}{\sqrt{4g^2 + \alpha^2}}|\varphi_1\rangle + \frac{2g}{\sqrt{4g^2 + \alpha^2}}|\varphi_a\rangle, \\ |E_2\rangle &= \frac{2g}{\sqrt{4g^2 + \alpha^2}}|\varphi_1\rangle - \frac{\alpha}{\sqrt{4g^2 + \alpha^2}}|\varphi_a\rangle, \\ |E_3\rangle &= \frac{\beta}{\sqrt{4g^2 + \beta^2}}|\varphi_2\rangle + \frac{2g}{\sqrt{4g^2 + \beta^2}}|\varphi_b\rangle, \\ |E_4\rangle &= \frac{2g}{\sqrt{4g^2 + \beta^2}}|\varphi_2\rangle - \frac{\beta}{\sqrt{4g^2 + \beta^2}}|\varphi_b\rangle, \\ |E_5\rangle &= -\sqrt{\frac{\sqrt{4g^2 + \Delta^2} - \Delta}{2\sqrt{4g^2 + \Delta^2}}}|\varphi_3\rangle + \sqrt{\frac{\sqrt{4g^2 + \Delta^2} + \Delta}{2\sqrt{4g^2 + \Delta^2}}}|\varphi_c\rangle, \\ |E_6\rangle &= \sqrt{\frac{\sqrt{4g^2 + \Delta^2} + \Delta}{2\sqrt{4g^2 + \Delta^2}}}|\varphi_3\rangle + \sqrt{\frac{\sqrt{4g^2 + \Delta^2} - \Delta}{2\sqrt{4g^2 + \Delta^2}}}|\varphi_c\rangle, \end{aligned} \quad (14)$$

where the coefficients are

$$\begin{aligned} \alpha &= \Delta + \sqrt{2}J - \sqrt{4g^2 + \Delta^2 + 2\sqrt{2}\Delta J + 2J^2}, \\ \beta &= \Delta - \sqrt{2}J - \sqrt{4g^2 + \Delta^2 - 2\sqrt{2}\Delta J + 2J^2}. \end{aligned} \quad (15)$$

Clearly, the qubit states $|100\rangle_a|000\rangle_c$ and $|001\rangle_a|000\rangle_c$ couple to the above eigenstates through two classical fields Ω_1 and Ω_3 . If the large detuning condition is satisfied, i.e. $\{|E_i|, |E_i - E_j|\} \gg \{|\Omega_1|, |\Omega_3|\}$, the effective coupling strength between $|100\rangle_a|000\rangle_c$ and $|001\rangle_a|000\rangle_c$ is

calculated by summing six independent-eigenstate transition channels. Most interestingly, if the one-photon detuning parameter Δ , the coupling strength between cavities J and the atom-cavity interacting constant meet the condition $\Delta = J = g$, a concise form of dipole-dipole interaction is obtained as

$$H_{eff}^1 = \frac{\Omega_1^2}{g}|100\rangle\langle 100| + \frac{\Omega_3^2}{g}|001\rangle\langle 001| + \frac{\Omega_1\Omega_3}{g}(|100\rangle\langle 001| + \text{H.c.}). \quad (16)$$

Likewise, the evolution of quantum states $|110\rangle_a|000\rangle_c$ and $|011\rangle_a|000\rangle_c$ are governed by

$$H_{eff}^2 = -\frac{\Omega_1^2}{2g}|110\rangle\langle 110| - \frac{\Omega_3^2}{2g}|011\rangle\langle 011| - \frac{\Omega_1\Omega_3}{2g}(|110\rangle\langle 011| + \text{H.c.}). \quad (17)$$

Eqs. (16) and (17) describe two kind of dipole-dipole interaction with different coupling constants. A permutation between states $|110\rangle_a|000\rangle_c$ and $|011\rangle_a|000\rangle_c$ is exactly followed by a cycle oscillation of state $|100\rangle_a|000\rangle_c$ or $|001\rangle_a|000\rangle_c$. The dynamical behaviors of states $|101\rangle_a|000\rangle_c$ and $|111\rangle_a|000\rangle_c$ are derived in the same way, but we do not need to consider their effects in the final effective Hamiltonian because the stark-shifts for them are cancelled due to the destructive interference in respective subspaces. Thus a selection of interaction time $T = g\pi/\Omega^2$ ($\Omega_1 = -\Omega_3 = \Omega$) will lead to the stand form of the Fredkin gate.

To illustrate the effectiveness of our approximation, we plot the population of each qubit state during the evolution in Fig. 3 with the full Hamiltonian (3), where the subplot (a) describes the conversion between states $|001\rangle_a|000\rangle_c$ and $|100\rangle_a|000\rangle_c$, (b) represents $|011\rangle_a|000\rangle_c$ and $|110\rangle_a|000\rangle_c$, and (c) and (d) depict the populations for states $|101\rangle_a|000\rangle_c$ and $|111\rangle_a|000\rangle_c$, respectively. It is unequivocal that the agreement between the effective and exact model is excellent under the given parameters and the data listed in the data cursor further validate the effectiveness of our approximation.

III. DISCUSSION AND EXPERIMENTAL FEASIBILITY

The average gate fidelity is introduced to qualify the performance of the Fredkin gate [43, 44]

$$\overline{F}(\varepsilon, U_{\text{FRED}}) = \frac{\sum_j \text{tr}[U_{\text{FRED}} U_j^\dagger U_{\text{FRED}}^\dagger \varepsilon(U_j)] + d^2}{d^2(d+1)}, \quad (18)$$

where $d = 8$ for three qubits and U_j being the tensor of Pauli matrices $III, IIX, IYY, \dots, ZZZ$, U_{FRED} being the ideal Fredkin gate and ε being the trace-preserving quantum operation obtained through our Fredkin gate.

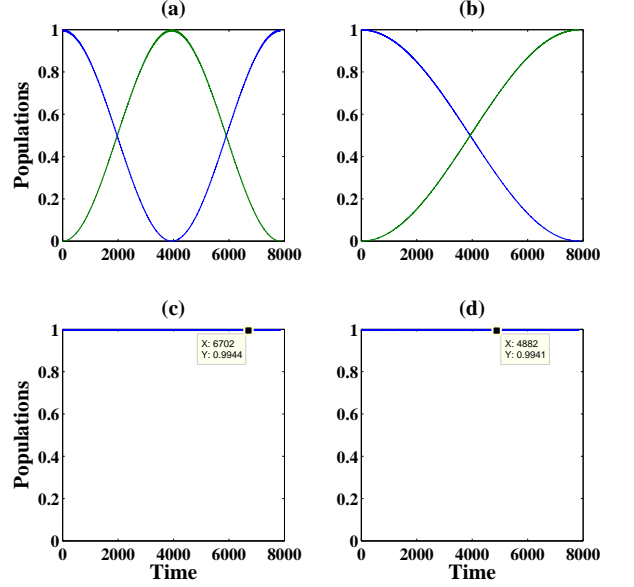


FIG. 3: (Color online) Evolution of the system from exact calculations of Hamiltonian Eq. (3). (a) these two curves represent the conversion of populations between states $|001\rangle$ and $|100\rangle$; (b) the populations of states $|011\rangle$ and $|110\rangle$; (c) the population of state $|101\rangle$; (d) the population of state $|111\rangle$. All cavities stay in vacuum states and the data listed in the data cursor further validate the effectiveness of our approximation. The relevant parameters are set as $\Omega_1 = -\Omega_3 = \Omega = 0.02g$, and $\Delta = J = g$. The dimensionless time is measured in the unit of g^{-1} .

In Fig. 4, we plot the relation between average gate fidelities for both resonant model and dispersive model versus the ratio $\Omega_{max}(\Omega)/g$, respectively. In the range of $0.02 \leq \Omega_{max}(\Omega)/g \leq 0.1$, the fidelity of resonant Fredkin gate keeps value much higher than 99%, while the fidelity for dispersive Fredkin gate decreases from 99.82% to 96% in an oscillation form. Now we pay attention to the decoherence effects on our Fredkin operation. In the model of coupled cavities, the typical dissipation channels include the spontaneous emission of atoms and the cavity decay. When these decoherence effects are taken into account and under the assumptions that the decay channels are independent, the master equation of the whole system can be expressed by the Lindblad form [42]

$$\dot{\rho} = -i[H_I, \rho] - \sum_{i=1}^3 \frac{\kappa}{2} (a_i^\dagger a_i \rho - 2a_i \rho a_i^\dagger + \rho a_i^\dagger a_i) - \sum_{j=0,1} \sum_{n=1}^3 \frac{\gamma_n^{ej}}{2} (\sigma_{ee}^n \rho - 2\sigma_{je}^n \rho \sigma_{ej}^n + \rho \sigma_{ee}^n), \quad (19)$$

where κ denotes the decay rate of the cavity, γ_n^{ej} represents the branching ration of the atomic decay from level $|e\rangle_n$ to $|j\rangle_n$ ($n = 1, 2, 3$) and we assume $\gamma_n^{e0} = \gamma_n^{e1} = \gamma/2$ for simplicity. The relation between the average fidelity

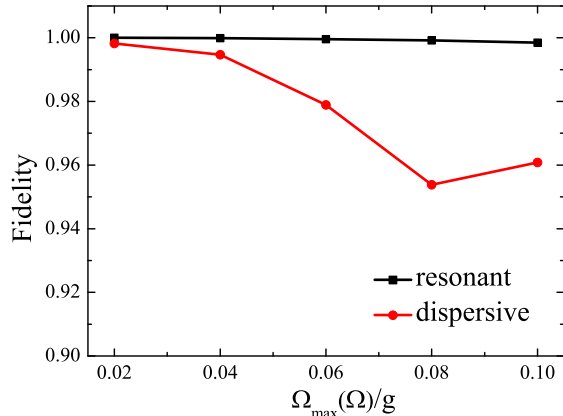


FIG. 4: (Color online) The average gate fidelity versus the Zeno requirement $\Omega_{max}(\Omega)/g$. The black curve represents the resonant model and the red curve corresponds to the dispersive model.

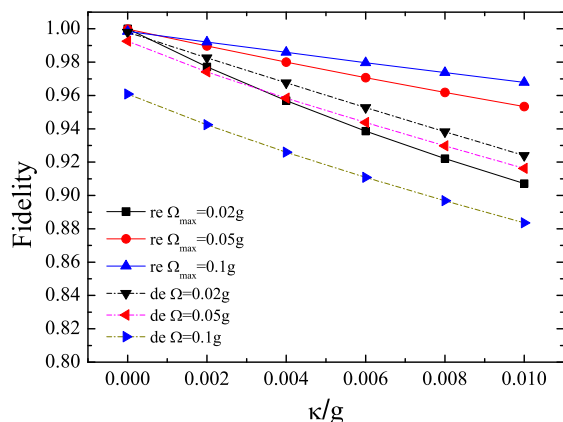


FIG. 5: (Color online) The average gate fidelities for resonant model and dispersive model versus decoherence parameter κ/g under three different driving lasers respectively, where we have set $\gamma = \kappa$ and $\Delta = J = g$.

ties and the decoherence parameter κ/g under three laser with different Rabi frequencies ($0.02g, 0.05g, 0.1g$) are manifested in Fig. 5. The solid lines relate to the resonant model and the dash-dot lines denotes the dispersive model. Comparing these two models within given parameters, we find that the fidelity obtained from the dispersive dynamics surpasses the resonant one only under a relatively weak driven laser (black line: $0.02g$). Thus, a resonant scheme is more realistic because a relatively strong Rabi frequency leads to a short interaction time, which makes the system avoid accumulation of decoher-

ence in time. In the absent of decay, we can achieve the maximal fidelities 99.98% and 99.80% for the resonant model ($\Omega_{max} = 0.05g$) and the dispersive model ($\Omega = 0.02g$), respectively. Even for a relatively large decay rate $\kappa = 0.01g$, the average fidelity remains above 95% for the resonant model and exceeds 92% for the dispersive model. In recent years, considerable progress has been made in fabrication of various high- Q microcavities including whispering-gallery-mode cavities [45, 46], micropost cavities and one- or two-dimensional photonic-crystal microcavities [47, 48], e.g. the strong interaction between atom and cavity has been predicted to be available in a toroidal microcavity system with the cavity mode wavelength of about 852 nm [46], where the quality factors in excess of 10^8 can be obtained corresponding to parameters $g \sim 2\pi \times 750$ MHz, $\gamma \sim 2\pi \times 2.62$ MHz, $\kappa \sim 2\pi \times 3.5$ MHz. In Ref. [49], large-scale arrays of ultrahigh- Q coupled nanocavities are also achieved with the parameters $(g, \gamma, \kappa) \sim (2.5 \times 10^9, 1.6 \times 10^7, 4 \times 10^5)$ Hz. By substituting these parameters into the Eqs. (18) and (19), we obtain the average fidelity of the Fredkin gate are 98.03% and 97.98% for the resonant case and 96.53% and 98.06% for the dispersive case, respectively. These values may not satisfy the condition for tolerating error threshold of about 10^{-5} [50], but they are relatively high in the sense of multi-qubit quantum information processing.

IV. SUMMARY

In summary, we have presented two efficient proposals for one-step implementation of the genuine Fredkin gate via trapping three identical atoms in a coupled-cavity array. The schemes need neither local operations nor ancillary levels and they are easily controlled and robust against the typical decoherence sources in cavity QED system. It is worth noting again that the dynamical characteristic discussed in the current scheme is particular in the coupled three-cavity array system, which is incapable to be simply duplicated in a single cavity. Our work may be useful for the quantum information processing in the near future.

ACKNOWLEDGMENT

This work is supported by Fundamental Research Funds for the Central Universities under Grant Nos. 11QNJJ009 and 12SSXM001, National Natural Science Foundation of China under Grant Nos. 11204028, 11175044, and 11074079, and National Research Foundation and Ministry of Education, Singapore (Grant No. WBS: R-710-000-008-271). X. Q. Shao is also supported in part by the Government of China through CSC.

-
- [1] P. W. Shor, "Algorithms for quantum computation: discrete logarithms and factoring," in *Proceedings of the 35th Symposium on Foundations of Computer Science, Santa Fe, 1994*, edited by S. Goldwasser (IEEE, Los Alamitos, CA, 1994), p. 124-134.
 - [2] P. W. Shor, "Polynomial-time algorithms for prime factorization and discrete logarithms on a quantum computer," *SIAM J. Comput.* **26**, 1484-1509 (1997).
 - [3] L. K. Grover, "Quantum computers can search rapidly by using almost any transformation," *Phys. Rev. Lett.* **80**, 4329-4332 (1998).
 - [4] D. P. DiVincenzo, "Two-bit gates are universal for quantum computation," *Phys. Rev. A* **51**, 1015 (1995).
 - [5] C. P. Yang and S. Han, " n -qubit-controlled phase gate with superconducting quantum-interference devices coupled to a resonator," *Phys. Rev. A* **72**, 032311 (2005).
 - [6] C. P. Yang and S. Han, "Realization of an n -qubit controlled- U gate with superconducting quantum interference devices or atoms in cavity QED," *Phys. Rev. A* **73**, 032317 (2006).
 - [7] T. Monz, K. Kim, W. Hänsel, M. Riebe, A. S. Villar, P. Schindler, M. Chwalla, M. Hennrich, and R. Blatt, "Realization of the quantum Toffoli gate with trapped ions," *Phys. Rev. Lett.* **102**, 040501 (2009).
 - [8] G. W. Lin, X. B. Zou, X. M. Lin, and G. C. Guo, "Robust and fast geometric quantum computation with multiqubit gates in cavity QED," *Phys. Rev. A* **79**, 064303 (2009).
 - [9] X. Q. Shao, H. F. Wang, L. Chen, S. Zhang, and K. H. Yeon, "One-step implementation of the Toffoli gate via quantum Zeno dynamics," *Phys. Lett. A* **374**, 28-33 (2009).
 - [10] X. Q. Shao, T. Y. Zheng, and S. Zhang, "Robust Toffoli gate originating from Stark shifts," *J. Opt. Soc. Am. B* **29**, 1203-1207 (2012).
 - [11] W. L. Yang, Z. Q. Yin, Z. Y. Xu, M. Feng, and J. F. Du, "One-step implementation of multiqubit conditional phase gating with nitrogen-vacancy centers coupled to a high-Q silica microsphere cavity" *Appl. Phys. Lett.* **96**, 241113 (2010).
 - [12] C. P. Yang, Y. X. Liu, and F. Nori, "Phase gate of one qubit simultaneously controlling n qubits in a cavity," *Phys. Rev. A* **81**, 062323 (2010).
 - [13] C. P. Yang, S. B. Zheng, and F. Nori, "Multiqubit tunable phase gate of one qubit simultaneously controlling n qubits in a cavity," *Phys. Rev. A* **82**, 062326 (2010).
 - [14] V. M. Stojanović, A. Fedorov, A. Wallraff, and C. Bruder, "Quantum-control approach to realizing a Toffoli gate in circuit QED," *Phys. Rev. B* **85**, 054504 (2012).
 - [15] A. M. Chen, S. Y. Cho, and M. D. Kim, "Implementation of a three-qubit Toffoli gate in a single step," *Phys. Rev. A* **85**, 032326 (2012).
 - [16] C. Jones, "Composite Toffoli gate with two-round error detection," *Phys. Rev. A* **87**, 052334 (2013).
 - [17] E. Fredkin and T. Toffoli, "Conservative logic," *Int. J. Theor. Phys.* **21**, 219 (1982).
 - [18] A. Barenco, A. Berthiaume, D. Deutsch, A. Ekert, R. Jozsa, and C. Macchiavello, "Stabilisation of quantum computations by symmetrisation," *SIAM J. Comput.* **26**, 1541-557 (1996).
 - [19] I. L. Chuang and Y. Yamamoto, "Simple quantum computer," *Phys. Rev. A* **52**, 3489 (1995).
 - [20] G. J. Milburn, "Quantum optical Fredkin gate," *Phys. Rev. Lett.* **62**, 2124-2127 (1989).
 - [21] J. Fiurásek, "Linear-optics quantum Toffoli and Fredkin gates," *Phys. Rev. A* **73**, 062313 (2006).
 - [22] J. Fiurásek, "Linear optical Fredkin gate based on partial-SWAP gate," *Phys. Rev. A* **78**, 032317 (2008).
 - [23] Y. X. Gong, G. C. Guo, and T. C. Ralph, "Methods for a linear optical quantum Fredkin gate," *Phys. Rev. A* **78**, 012305 (2008).
 - [24] Q. Lin and J. Li, "Quantum control gates with weak cross-Kerr nonlinearity," *Phys. Rev. A* **79**, 022301 (2009).
 - [25] Q. Lin and B. He, "Single-photon logic gates using minimal resources," *Phys. Rev. A* **80**, 042310 (2009).
 - [26] X. B. Zou, J. Kim, and H. W. Lee, "Generation of two-mode nonclassical motional states and a Fredkin gate operation in a two-dimensional ion trap," *Phys. Rev. A* **63**, 065801 (2001).
 - [27] B. Wang and L. M. Duan, "Implementation scheme of controlled SWAP gates for quantum fingerprinting and photonic quantum computation," *Phys. Rev. A* **75**, 050304(R) (2007).
 - [28] J. Song, Y. Xia, and H. S. Song, "Quantum gate operations using atomic qubits through cavity input-output process," *Europhys. Lett.* **87**, 50005 (2009).
 - [29] S. B. Zheng, "Implementation of Toffoli gates with a single asymmetric Heisenberg XY interaction," *Phys. Rev. A* **87**, 042318 (2013).
 - [30] X. Q. Shao, T. Y. Zheng, and S. Zhang, "Fast synthesis of the Fredkin gate via quantum Zeno dynamics," *Quant. Inf. Proc.* **11**, 1797-1808 (2012).
 - [31] D. G. Angelakis, M. F. Santos, and S. Bose, "Photon-blockade-induced Mott transitions and XY spin models in coupled cavity arrays," *Phys. Rev. A* **76**, 031805(R) (2007).
 - [32] E. K. Irish, C. D. Ogden, and M. S. Kim, "Polaritonic characteristics of insulator and superfluid states in a coupled-cavity array," *Phys. Rev. A* **77**, 033801 (2008).
 - [33] J. Cho, D. G. Angelakis, and S. Bose, "Fractional quantum Hall state in coupled cavities," *Phys. Rev. Lett.* **101**, 246809 (2008).
 - [34] T. C. H. Liew, and V. Savona, "Multimode entanglement in coupled cavity arrays," *New J. Phys.* **15**, 025015 (2013).
 - [35] M. J. Hartmann, F. G. S. Brandão, and M. B. Plenio, "Quantum many-body phenomena in coupled cavity arrays," *Laser Photon. Rev.* **2**, 527 (2008), and reference therein.
 - [36] A. Serafini, S. Mancini, and S. Bose, "Distributed quantum computation via optical fibers," *Phys. Rev. Lett.* **96**, 010503 (2006).
 - [37] Z. Q. Yin and F. L. Li, "Multiatom and resonant interaction scheme for quantum state transfer and logical gates between two remote cavities via an optical fiber," *Phys. Rev. A* **75**, 012324 (2007).
 - [38] Z. B. Yang, H. Z. Wu, W. J. Su, and S. B. Zheng, "Quantum phase gates for two atoms trapped in separate cavities within the null- and single-excitation subspaces," *Phys. Rev. A* **80**, 012305 (2009).
 - [39] Z. B. Yang, Y. Xia, S. B. Zheng, "Resonant scheme for realizing quantum phase gates for two separate atoms via

- coupled cavities,” *Opt. Commun.* **283**, 3052-3057 (2010).
- [40] P. Facchi and S. Pascazio, “Quantum Zeno dynamics of a field in a cavity,” *Phys. Rev. Lett.* **89**, 080401 (2002).
 - [41] A. Beige, H. Cable, C. Marr, P. L. Knight, “Speeding up gate operations through dissipation,” *Laser Phys.* **15**, 162-169 (2005).
 - [42] M. O. Scully and M. S. Zubairy, *Quantum Optics* (Cambridge University Press, Cambridge, 1997).
 - [43] A. G. White, A. Gilchrist, G. J. Pryde, J. L. O’Brien, M. J. Bremner, and N. K. Langford, “Measuring two-qubit gates,” *J. Opt. Soc. Am. B* **24**, 172-183 (2007).
 - [44] M. A. Nielsen, “A simple formula for the average gate fidelity of a quantum dynamical operation,” *Phys. Lett. A* **303**, 249 (2002).
 - [45] D. K. Armani, T. J. Kippenberg, S. M. Spillane, and K. J. Vahala, “Ultra-high- Q toroid microcavity on a chip,” *Nature* **421**, 925-928 (2003).
 - [46] S. M. Spillane, T. J. Kippenberg, K. J. Vahala, K. W. Goh, E. Wilcut, and H. J. Kimble, “Ultrahigh- Q toroidal microresonators for cavity quantum electrodynamics,” *Phys. Rev. A* **71**, 013817 (2005).
 - [47] B. S. Song, S. Noda, T. Asano, and Y. Akahane, “Ultra-high- Q photonic double-heterostructure nanocavity,” *Nature Mater.* **4**, 207-210 (2005).
 - [48] T. Tanabe, M. Notomi, E. Kuramochi, A. Shinya, and H. Taniyama, “Trapping and delaying photons for one nanosecond in an ultrasmall high- Q photonic-crystal nanocavity,” *Nature Photon.* **1**, 49-52 (2007).
 - [49] M. Notomi, E. Kuramochi, and T. Tanabe, “Large-scale arrays of ultrahigh- Q coupled nanocavities,” *Nat. Photonics* **2**, 741 (2008).
 - [50] J. Preskill, Lecture Notes on Quantum Computation, see <http://www.theory.caltech.edu/people/preskill/ph229>.